arXiv:1606.01494v1 [astro-ph.HE] 5 Jun 2016

Received 2015 November 22; accepted 2016 June 2

On the thermal line emission from the outflows in ultraluminous X-ray sources

Ya-Di Xu[1], and Xinwu Cao [2,3]

ABSTRACT

The atomic features in the X-ray spectra of the ultraluminous X-ray source (ULX) may be associated with the outflow (Middleton et al. 2015), which may provide a way to explore the physics of the ULXs. We construct a conical outflow model, and calculate the thermal X-ray Fe emission lines from the outflows. Our results show that thermal line luminosity decreases with increasing outflow velocity or/and opening angle of the outflow for a fixed kinetic power of the outflows. Assuming the kinetic power of the outflows to be comparable with the accretion power in the ULXs, we find that the equivalent width can be several eV for the thermal X-ray Fe emission line from the outflows in the ULXs with stellar mass black holes. The thermal line luminosity is proportional to $1/M_{\rm bh}$ ($M_{\rm bh}$ is the black hole mass of the ULX). The equivalent width decreases with the black hole mass, which implies that the Fe line emission from the outflows can hardly be detected if the ULXs contain intermediate mass black holes. Our results suggest that the thermal X-ray Fe line emission should be preferentially be detected in the ULXs with high kinetic power slowly moving outflows from the accretion disks surrounding stellar mass black holes/neutron stars. The recent observed X-ray atomic features of the outflows in the ULX may imply that it contains a stellar mass black hole/neutron star (Pinto et al. 2016).

Subject headings: accretion, accretion disks; black hole physics; X-rays: binaries; ISM: jets and outflows; radiation mechanisms: thermal

[1]Department of Physics and Astronomy, Shanghai Jiao Tong University, 800 Dongchuan Road, Shanghai 200240, China ydxu@sjtu.edu.cn

[2]SHAO-XMU Joint Center for Astrophysics, Shanghai Astronomical Observatory, Chinese Academy of Sciences, 80 Nandan Road, Shanghai, 200030, China; cxw@shao.ac.cn

[3]Key Laboratory of Radio Astronomy, Chinese Academy of Sciences, 210008 Nanjing, China

1. Introduction

The nature of ultraluminous X-ray sources (ULXs) is still unclear mainly due to the lack of dynamical mass determination of their central sources, though progress has been achieved in recent years (Liu et al. 2013; Motch et al. 2014). This makes it difficult to resolve the accretion mode in ULXs (see Fabrika et al. 2016, for a review, and the references theirin). The ULXs may either be powered by accretion on to stellar mass black holes at high rates, or associated with accretion at ∼Eddington rates on to intermediate mass black holes with $M_{\rm bh} \gtrsim 100{\rm M}_{\odot}$. There is evidence of accretion on to stellar mass black holes in some individual ULXs (Liu et al. 2013; Motch et al. 2014), though the nature of the compact objects in most of the ULXs is somewhat ambiguous.

The super-Eddington accretion on to a stellar mass black hole in the ULX can be an analogy with SS433, a well known super critical accreting source in our galaxy (e.g., Fabrika & Mescheryakov 2001; Fabrika 2004). The Doppler shifted X-ray emission lines have been observed in the X-ray spectra of SS433, which are supposed to be emitted from the jets (Watson et al. 1986; Kotani et al. 1994, 1996; Marshall et al. 2013). The X-ray line emission from the jets implies a baryonic component in the jets (Díaz Trigo et al. 2013), which strongly supports the Blandford-Payne jet formation mechanism at least for this source (Blandford & Payne 1982). A radio-X-ray correlation in Cygnus X-1 is found to extend to the high/soft state only if its hard X-ray emission is considered (after subtracting the blackbody component emitted from the thin disk) (Zdziarski et al. 2011). A similar feature has been found in active galactic nuclei (Wu et al. 2013). These imply that the jet formation may probably be related to the hot coronae above the thin disks (Merloni & Fabian 2002; Cao 2004; Zdziarski et al. 2011; Wu et al. 2013). The calculations of magnetically accelerated outflows show that hot gas (probably in the corona) is necessary for launching an outflow from the radiation-pressure-dominated accretion disk (Cao 2014). If this is the case, a fraction of the hot ions and electrons in the corona may be driven into the jets/outflows by the magnetic field of the disk. The gas in the jets/outflows with suitable temperature may emit X-ray lines mainly due to the re-combination of the ions and elections in the jets.

The observed Doppler-shifted X-ray emission lines provide useful constraints on the properties of the jets in SS433 (Kotani et al. 1996; Marshall et al. 2013). It was claimed that the Doppler shifted X-ray lines had been detected in the X-ray binary 4U 1630−47 (Cui et al. 2000; Díaz Trigo et al. 2013), though it was not confirmed (Neilsen et al. 2014). The X-ray observation of the ULX NGC 1313 X-1 provides evidence of soft X-ray atomic features associated with the winds or outflows (Middleton et al. 2015; Pinto et al. 2016). The thermal X-ray line emission from the outflows may provide useful clues on the nature of ULXs.

In this work, we calculate the thermal X-ray line emission from the outflows in ULXs, and show how the physical properties of the outflows are related to the X-ray line emission. We describe the outflow model in Section 2, and the calculations of the thermal X-ray line emission in Section 3. Sections 4 and 5 contain the results and discussion.

2. Outflow model

The gas in the corona above a thin disk is very hot. The temperature of the ions in the corona is nearly virialized ($\sim 10^{11-12}$K in the inner region of the disk), which is much higher than the electron temperature ($\sim 10^{9}$K) (e.g., Merloni & Fabian 2002; Liu et al. 2003; Cao 2009). A small fraction of the hot gas in the corona may probably accelerated into the outflows by the magnetic field co-rotating with the gas in the disk or/and the radiation force of the disk (Cao 2014). The calculations of the outflow acceleration is rather complicated (Cao 2014), which is beyond the scope of this work. Here, we adopt a simplified model of the outflows with a conical geometry (see Cao 2010, for the details).

The density of a conical outflow at a distance of R from the black hole is

$$\rho(R) = \frac{\dot{M}_{\rm w}}{4\pi R^2 \gamma_{\rm w} \beta_{\rm w} c (1-\cos\theta_{\rm w}/2)}, \tag{1}$$

where $\dot{M}_{\rm w}$ is the mass loss rate of a pair of outflows, $\theta_{\rm w}$ is the opening angle of the conical outflows, $\beta_{\rm w} = v_{\rm w}/c$ is the bulk radial velocity of the outflows, and

$$\gamma_{\rm w} = \frac{1}{(1-\beta_{\rm w}^2)^{1/2}}. \tag{2}$$

The outflow expanding adiabatically is a good approximation, which leads to $T \propto R^{-4/3}$ (see Cao 2010, for the detailed calculations, but for the outflow with a constant velocity along R in this work). The kinetic power of the outflows can be calculated with

$$P_{\rm kin} = (\gamma_{\rm w} - 1)\dot{M}_{\rm w} c^2, \tag{3}$$

where $r = R/R_{\rm S}$, $R_{\rm S} = 2GM_{\rm bh}/c^2$, and $m = M_{\rm bh}/M_{\odot}$. Substitute Equation (3) into Equation (1), we have

$$n_{\rm e}(r) = 1.77\times10^{-20} m^{-2} P_{\rm kin} (\gamma_{\rm w}-1)^{-1} \gamma_{\rm w}^{-1} \beta_{\rm w}^{-1} r^{-2} \left(1-\cos\frac{\theta_{\rm w}}{2}\right)\ {\rm cm}^{-3}. \tag{4}$$

As the gas in the outflows is driven from the corona, only a small fraction of the electrons may be re-accelerated in shocks to a non-thermal component, and the outflows should contain

a dominant component of thermal gas. In this work, we assume a power-law R-dependent electron temperature in the outflows,

$$T_{\rm e}(R) = T_{\rm e,in}\left(\frac{R}{R_{\rm in}}\right)^{-\xi_{\rm T}}, \tag{5}$$

where $R_{\rm in}$ is the location of the base of the outflows, and the thermal electron temperature is $T_{\rm e,in}$ at $R = R_{\rm in}$. For an adiabatically expanding outflow, the index $\xi_{\rm T} = 4/3$ (Cao 2010).

3. Thermal X-ray line emission from the outflows

The thermal X-ray line emissions from the outflows can be calculated, when the temperature, density, and metallicity of the gas, are specified. Using the outflow model described in Sect. 2, we can calculate the thermal X-ray line emissions from the outflows. The total line luminosity emitted from the outflows, $L_{\rm line}$, can be calculated by integrating over R in the outflows,

$$L_{\rm line} = \frac{Z}{Z_\odot}\int_{R_{\rm in}}^{R_{\rm out}} \epsilon[T_{\rm e}(R)] n_{\rm e,th}^2(R) 4\pi R^2 \left(1-\cos\frac{\theta_{\rm w}}{2}\right) {\rm d}R, \tag{6}$$

where $R_{\rm in}$ is the location of the jet base, $n_{\rm e,th}$ is the density of the thermal electrons, and Z is the metallicity of the gas. Substitute Equation (4) into Equation (6), we derive the line luminosity,

$$L_{\rm line} = 1.01\times10^{-22} m^{-1} P_{\rm kin}^2 (\gamma_{\rm w}-1)^{-2}\gamma_{\rm w}^{-2}\beta_{\rm w}^{-2}\left(1-\cos\frac{\theta_{\rm w}}{2}\right)^3 f_{\rm th}^2\left(\frac{Z}{Z_\odot}\right) \times \int_{r_{\rm in}}^{r_{\rm out}} \epsilon[T_{\rm e}(r)] r^{-2} dr \ {\rm erg\ s^{-1}}, \tag{7}$$

where a parameter $f_{\rm th}$ is used to describe the fraction of the thermal electrons in the outflows, i.e., $n_{\rm e,th} = f_{\rm th} n_{\rm e}$. The line emissivity ϵ as a function of temperature is calculated with the standard software package Astrophysical Plasma Emission Code (APEC)(Smith et al. 2001) assuming the solar metallicity. The code has been used to calculate the X-ray emission lines emitted from the accretion disk/corona systems (e.g., Narayan & Raymond 1999; Perna et al. 2000; Xu et al. 2006; Xu 2013). The collisional excitation, recombination to excited levels and dielectronic satellite lines have been included in APEC code (see Smith et al. 2001, for the details). Assuming ionization equilibrium in the plasma, we can thus calculate the total line luminosities of the X-ray line emissions with the structure (e.g., temperature and density) of the outflows.

4. Results

The structure of the outflow is available when the black hole mass $M_{\rm bh}$, the kinetic power of the outflows $P_{\rm kin}$, the outflow velocity $\beta_{\rm w}$, and the opening angle of the outflow $\theta_{\rm w}$ are specified (see Sect. 2). The thermal line luminosity can be calculated with the derived outflow structure by using the standard software package Astrophysical Plasma Emission Code (APEC)(Smith et al. 2001). The electron temperature $T_{\rm e,in} = 10^9$ K at the base of the outflow $R_{\rm in} = 5R_{\rm S}$ are adopted in most of the calculations. In this work, the fraction of the thermal electrons in the outflows $f_{\rm th} = 0.9$ is used, the precise value of which will not affect much on the main results of this work. The solar metallicity is adopted in all of the calculations. In Figure 1, we plot the thermal line luminosities as functions of the outflow velocity $\beta_{\rm w}$. The dependence of the line luminosity with the opening angle of the outflow $\theta_{\rm w}$ is plotted in Figure 2.

In order to calculate the equivalent width of the X-ray emission line, we need to know the X-ray continuum spectrum of the ULX. In this work, a typical template spectrum, of which the photon spectral index $\Gamma = 2$ for the 2−10 keV power law spectrum, is adopted. The fraction of the X-ray luminosity in 2−10 keV to the bolometric luminosity is roughly taken as 0.2 similar to X-ray binaries (e.g., Díaz Trigo et al. 2013). Assuming the accretion power $L_{\rm acc} = P_{\rm kin}$, we calculate the equivalent widths of the lines as functions of $\beta_{\rm w}$ in Figure 3. The equivalent widths varying with the opening angle of the outflow $\theta_{\rm w}$ is given in Figure 4. The thermal line emission is sensitively dependent of the temperature of the outflows. In Figure 5, we plot the equivalent widths as functions of the electron temperature of the gas at the base of the outflows.

5. Discussion

The thermal line emission is proportional to $n_{\rm e}^2$ (see Equation 6), and $P_{\rm kin} \propto n_{\rm e}$, so the thermal X-ray line luminosity $L_{\rm line} \propto P_{\rm kin}^2$. The thermal line luminosity $L_{\rm line} \propto m^{-1}$ (see Equation 7), which indicates that the line emission may more easily be detected in the sources with smaller black hole masses or/and higher kinetic-power-outflows. The electron density $n_{\rm e} \propto R^{-2}$ for a conical outflow, i.e., the electron number density decreases with increasing R, and therefore the thermal line luminosity $L_{\rm line}$ decreases with increasing $R_{\rm in}$. Similarly, the thermal X-ray line luminosity decreases with increasing opening angle of the conical outflows for a fixed kinetic power of the outflows. In order to estimate the observed equivalent widths of the thermal X-ray emission lines, we use a template X-ray continuum spectrum of the disk. The continuum luminosity is assumed to be proportional to the accretion power $L_{\rm acc}$, so the observed equivalent width, EW $\propto L_{\rm line}/L_{\rm acc} \propto P_{\rm kin}$, for a given ratio $P_{\rm kin}/L_{\rm acc}$, because

$L_{\rm line} \propto m^{-1}$.

The emissivity of the Fe Kα line varies with the electron temperature. We explore how the equivalent widths vary with the electron temperature $T_{\rm e,in}$ at the base of the outflows (see Figure 5). We find that the equivalent widths are large when the temperature of the electrons at the base of the outflows is $\sim 10^{8-9}$ K. The equivalent widths of the iron lines can be ~ 1 eV even for the outflows with an opening angle $\theta_{\rm w} = 45^\circ$ in the ULX containing a stellar mass black hole with $M_{\rm bh} = 10 M_\odot$, while it decreases to $\lesssim 0.1$ eV for a black hole mass with $M_{\rm bh} \gtrsim 100 M_\odot$. This means that the line emission from the outflows sensitively depends on the black hole mass, because the size of the outflow is proportional to the black hole mass, and the density of the gas $n_{\rm e} \propto 1/M_{\rm bh}$. The equivalent widths of the Fe Kα lines depend on outflow velocity sensitively (see Figures 1 and 3). The line luminosity $L_{\rm line} \propto \beta_{\rm w}^{-6}$ for a non-relativistic outflow, i.e., $\gamma_{\rm w} \rightarrow 1$ in Equation (7). It means that the equivalent widths can be higher for the outflows with a lower velocity. If the outflow velocity $\beta_{\rm w} = 0.2$, the equivalent widths of the Fe Kα lines would be around 10 eV. The equivalent widths of the soft X-ray atomic lines from the outflow in the ULX NGC 1313 X-1 are $\sim 0.01 - 0.17$ keV (Middleton et al. 2015). It was suggested that some ULXs may contain neutron stars (King & Lasota 2016). Our model can also be applied for the outflows driven from the accretion disk surrounding a neutron star, its line luminosity can be several times higher than that for a stellar black hole case for the same kinetic power of the outflows, because $L_{\rm line} \propto 1/M$. The equivalent widths equivalent widths of the Fe Kα lines can be as high as several tens of eV for the ULX containing a neutron star.

We have not considered the line profile in our calculations. The ion temperature Ti $\sim 10^{11-12}$K of the corona in the inner region of the disk, so the ion temperature of the gas at the base of the outflows Ti $\lesssim 10^{11-12}$K. The widths of the Fe Kα lines due to thermal broadening are $\lesssim 0.2 - 0.6$ keV. For the outflows magnetically driven from the disk, the gas in the outflows is also rotating (Spruit 2010). If the outflow is viewed edge-on, the line broadening due to rotation of the gas in the outflow is ~ 0.25 keV (for $v_{\rm w} = 0.2$c) assuming the rotating velocity to be an order of magnitude lower than the radial velocity (Spruit 2010). This means that the rotational broadening of the iron Kα emission line is roughly at the same order of the thermal broadening.

The dynamics of the outflows has not been considered in this work. A simplified model of an outflow with a constant radial velocity is adopted in this work. We take the outflow velocity of as a model parameter. The realistic outflow may experience re-acceleration, and its velocity may vary with the distance from the black hole. The Fe Kα line luminosity for such an outflow can be roughly estimated by interpolation of the results of the outflows with constant velocities presented in this work.

For the relativistic jets, the line emission may be strongly beamed if it is viewed at a small angle with line of sight, however, the line emission decreases significantly with increasing jet velocity for a fixed kinetic jet power (see Figures 1 and 3). In this work, we focus on the slowly moving outflows, and we have not considered the Doppler beaming effect in our calculations, which will not affect our main conclusions.

In this work, the ratio $P_{\rm kin}/L_{\rm acc} = 1$ is adopted in our calculations, though the values of the ratios are quite unclear for the ULXs. If it is significantly lower than unity, the thermal line emission from the outflows can hardly be detected even if the ULX contains a stellar mass black hole. The ratio of the jet power to the accretion power for active galactic nuclei (AGN) has been extensively studied, which shows the jet power is roughly comparable with the accretion power in most radio-loud AGNs, and the jet power can be significantly higher than the accretion power in some luminous radio galaxies (e.g., Gu et al. 2009; Fernandes et al. 2011; McNamara et al. 2011; Ghisellini et al. 2014). Recently, a thin accretion disk with magnetically driven jets is suggested to explain extremely powerful jets observed in some radio galaxies (Li 2014). For a conventional thin disk, almost all the kinetic energy of the rotating gas in the disk is dissipated in the disk and is radiated out locally. When the magnetically driven jets are present, a fraction of the kinetic energy/angular momentum of the disk is removed from the disk by the jets, and the remainder is dissipated in the disk. An ideal extreme case is an dissipateless accretion disk can be purely driven by magnetic jets/outflows, i.e., all the rotating energy of the gas in the disk is tapped into the jets/outflows. If most gravitational energy and angular momentum of the disk is carried away in the jets, and therefore the jet power can be much higher than the accretion power (see Li 2014, for the details). We believe such mechanism may also work in the accretion-outflow systems of the ULXs, if the outflow is driven with the Blandford-Payne mechanism.

The solar metallicity $Z = Z_{\odot}$ is adopted in our calculations (see Section 4). We note that the X-ray thermal line emission is proportional to the metallicity (see Equation 6). It is shown that the dispersion of the metallicity of the stars in our galaxy is ~ 0.5 dex (e.g., Chen et al. 2003, 2004, 2008; Huang et al. 2015). The metallicity of nearby galaxies does not deviate much from the solar value (e.g., Perelmuter et al. 1995; Kong et al. 2000; Kudritzki et al. 2012; Magrini et al. 2016). This means that our results may not be altered much by the metallicity.

In summary, our results suggest that the thermal X-ray Fe line emission should be preferentially be detected in the ULXs with high kinetic power outflows from the accretion disks surrounding stellar mass black holes/neutron stars, or the X-ray atomic features of the outflows may strongly suggest a stellar mass black hole in the ULX (Middleton et al. 2015; Pinto et al. 2016).

We thank the referee for his/her very helpful comments/suggestions on the manuscript. This work is supported by the NSFC (grants 11233006, and 11220101002). the Strategic Priority Research Program the Emergence of Cosmological Structures of the CAS (grant No. XDB09000000), and Shanghai Municipality.

REFERENCES

Blandford, R. D., & Payne, D. G. 1982, MNRAS, 199, 883

Cao, X. 2004, ApJ, 613, 716

Cao, X. 2009, MNRAS, 394, 207

Cao, X. 2010, ApJ, 724, 855

Cao, X. 2014, ApJ, 783, 51

Chen, L., Hou, J. L., & Wang, J. J. 2003, AJ, 125, 1397

Chen, L., Hou, J. L., & Wang, J. J. 2004, Recycling Intergalactic and Interstellar Matter, 217, 194

Chen, L., Hou, J. L., Zhao, J. L., & de Grijs, R. 2008, IAU Symposium, 248, 433

Cui, W., Chen, W., & Zhang, S. N. 2000, ApJ, 529, 952

Díaz Trigo, M., Miller-Jones, J. C. A., Migliari, S., Broderick, J. W., & Tzioumis, T. 2013, Nature, 504, 260

Fabrika, S. 2004, Astrophysics and Space Physics Reviews, 12, 1

Fabrika, S., & Mescheryakov, A. 2001, Galaxies and their Constituents at the Highest Angular Resolutions, 205, 268

Fabrika, S., Vinokurov, A., & Atapin, K. 2016, arXiv:1601.05971

Fernandes, C. A. C., Jarvis, M. J., Rawlings, S., et al. 2011, MNRAS, 411, 1909

Ghisellini, G., Tavecchio, F., Maraschi, L., Celotti, A., & Sbarrato, T. 2014, Nature, 515, 376

Gu, M., Cao, X., & Jiang, D. R. 2009, MNRAS, 396, 984

Huang, Y., Liu, X.-W., Zhang, H.-W., et al. 2015, Research in Astronomy and Astrophysics, 15, 1240

King, A., & Lasota, J.-P. 2016, MNRAS, 458, L10

Kong, X., Zhou, X., Chen, J., et al. 2000, AJ, 119, 2745

Kotani, T., Kawai, N., Aoki, T., et al. 1994, PASJ, 46, L147

Kotani, T., Kawai, N., Matsuoka, M., & Brinkmann, W. 1996, PASJ, 48, 619

Kudritzki, R.-P., Urbaneja, M. A., Gazak, Z., et al. 2012, ApJ, 747, 15

Li, S.-L. 2014, ApJ, 788, 71

Liu, B. F., Mineshige, S., & Ohsuga, K. 2003, ApJ, 587, 571

Liu, J.-F., Bregman, J. N., Bai, Y., Justham, S., & Crowther, P. 2013, Nature, 503, 500

Magrini, L., Coccato, L., Stanghellini, L., Casasola, V., & Galli, D. 2016, A&A, 588, A91

Marshall, H. L., Canizares, C. R., Hillwig, T., et al. 2013, ApJ, 775, 75

McNamara, B. R., Rohanizadegan, M., & Nulsen, P. E. J. 2011, ApJ, 727, 39

Merloni, A., & Fabian, A. C. 2002, MNRAS, 332, 165

Middleton, M. J., Walton, D. J., Fabian, A., et al. 2015, MNRAS, 454, 3134

Motch, C., Pakull, M. W., Soria, R., Grisé, F., & Pietrzyński, G. 2014, Nature, 514, 198

Narayan, R., & Raymond, J. 1999, ApJ, 515, L69

Neilsen, J., Coriat, M., Fender, R., et al. 2014, ApJ, 784, L5

Perelmuter, J.-M., Brodie, J. P., & Huchra, J. P. 1995, AJ, 110, 620

Perna, R., Raymond, J., & Narayan, R. 2000, ApJ, 541, 898

Pinto, C., Middleton, M. J., & Fabian, A. C. 2016, Nature, 533, 64

Smith, R. K., Brickhouse, N. S., Liedahl, D. A., Raymond, J. C. 2001, ApJ, 556, L91

Spruit, H. C. 2010, Lecture Notes in Physics, Berlin Springer Verlag, 794, 233

Watson, M. G., Stewart, G. C., King, A. R., & Brinkmann, W. 1986, MNRAS, 222, 261

Wu, Q., Cao, X., Ho, L. C., & Wang, D.-X. 2013, ApJ, 770, 31

Xu, Y.-D. 2013, ApJ, 763, 75

Xu, Y.-D., Narayan, R., Quataert, E., Yuan, F., & Baganoff, F. K. 2006, ApJ, 640, 319

Zdziarski, A. A., Skinner, G. K., Pooley, G. G., & Lubiński, P. 2011, MNRAS, 416, 1324

This preprint was prepared with the AAS LaTeX macros v5.2.

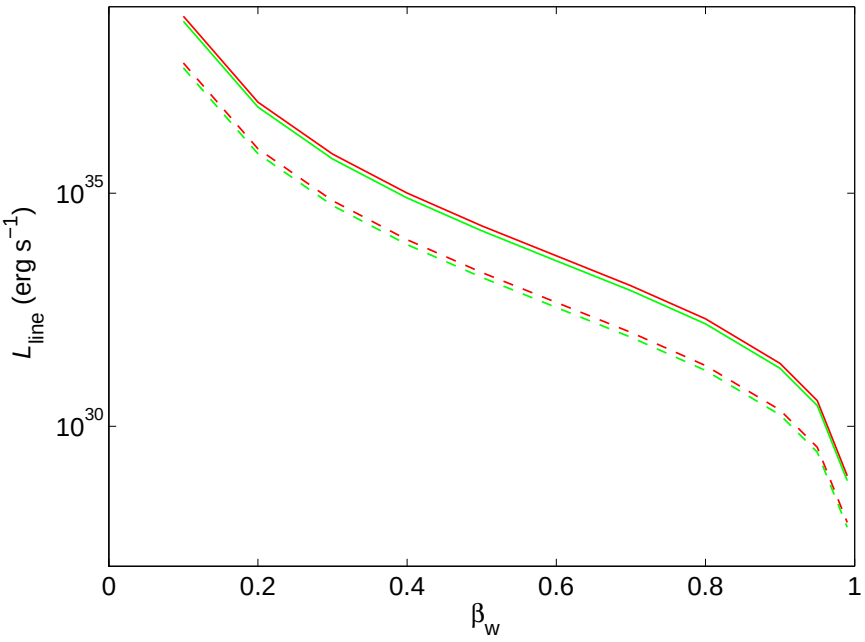

Fig. 1.— The luminosities of the line emitted from the outflows as functions of the outflow velocity. The kinetic power $P_{\rm kin} = 10^{39}$ erg s^{-1}, and the opening angle $\theta_{\rm w} = 5^\circ$ of the outflows are adopted in the calculations. The red lines are the luminosities of the Fe XXVI Kα emission line for the outflows, while the green lines are the Fe XXV Kα emission line luminosity. The solid lines represent the results calculated with $M_{\rm bh} = 10M_\odot$, while the dashed lines are for $M_{\rm bh} = 100M_\odot$.

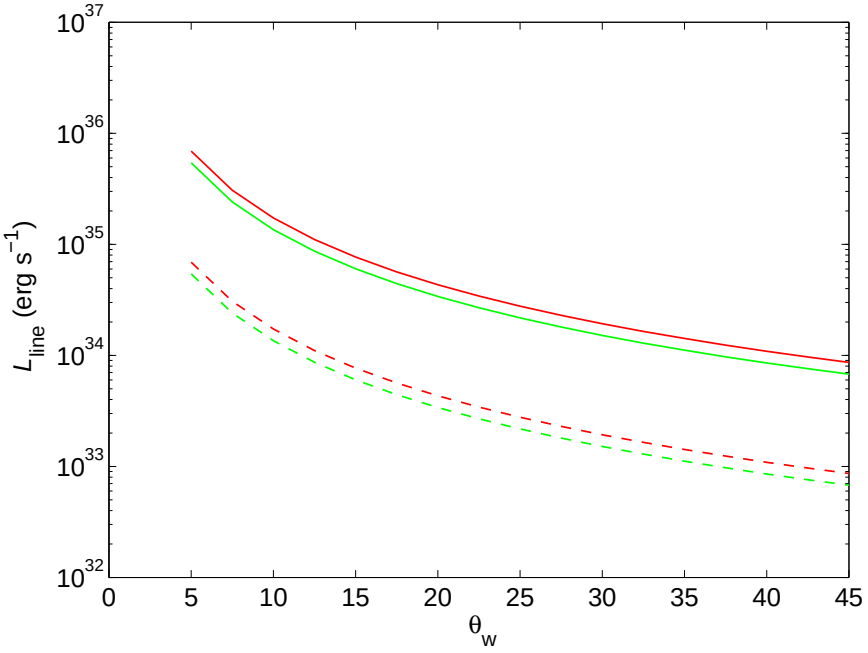

Fig. 2.— The luminosities of the line emitted from the outflows as functions of the opening angle $\theta_{\rm w}$ of the outflows. The kinetic power of the outflows $P_{\rm kin} = 10^{39}$ erg s^{-1}, and the outflow velocity $\beta_{\rm w} = 0.3$, are adopted in the calculations. The red lines are the luminosities of the Fe XXVI Kα emission line for the outflows, while the green lines are the Fe XXV Kα emission line luminosity. The solid lines represent the results calculated with $M_{\rm bh} = 10M_{\odot}$, while the dashed lines are for $M_{\rm bh} = 100M_{\odot}$.

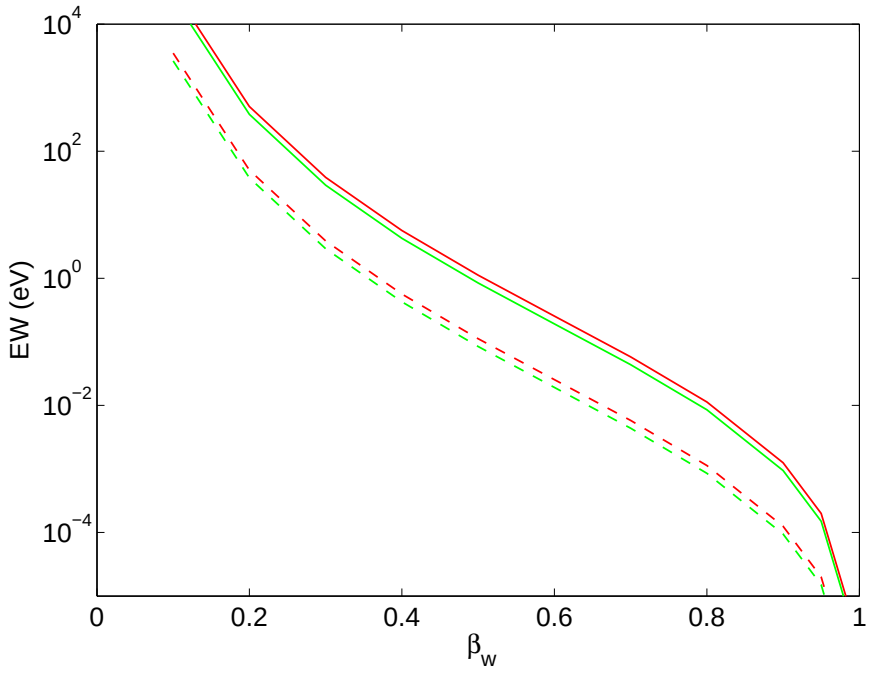

Fig. 3.— The equivalent widths of the line emission as functions of the outflow velocity. The accretion power $L_{\rm acc} = P_{\rm kin} = 10^{39}$ erg s^{-1}, and the opening angle $\theta_{\rm w} = 5^\circ$ are adopted in the calculations. The red lines are the luminosities of the Fe XXVI Kα emission line for the outflows, while the green lines are the Fe XXV Kα emission line luminosity. The solid lines represent the results calculated with $M_{\rm bh} = 10 M_\odot$, while the dashed lines are for $M_{\rm bh} = 100 M_\odot$.

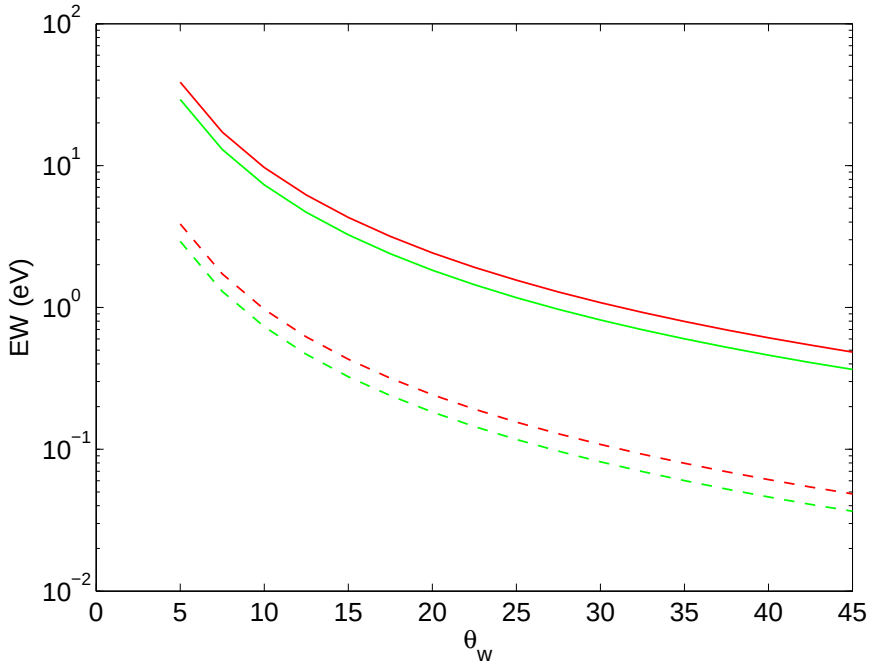

Fig. 4.— The equivalent widths of the line emitted from the outflows as functions of the opening angle $\theta_{\rm w}$ of the outflows. The accretion power $L_{\rm acc} = P_{\rm kin} = 10^{39}$ erg s^{-1}, and the outflow velocity $\beta_{\rm w} = 0.3$, are adopted in the calculations. The red lines are the luminosities of the Fe XXVI Kα emission line for the outflows, while the green lines are the Fe XXV Kα emission line luminosity. The solid lines represent the results calculated with $M_{\rm bh} = 10 M_{\odot}$, while the dashed lines are for $M_{\rm bh} = 100 M_{\odot}$.

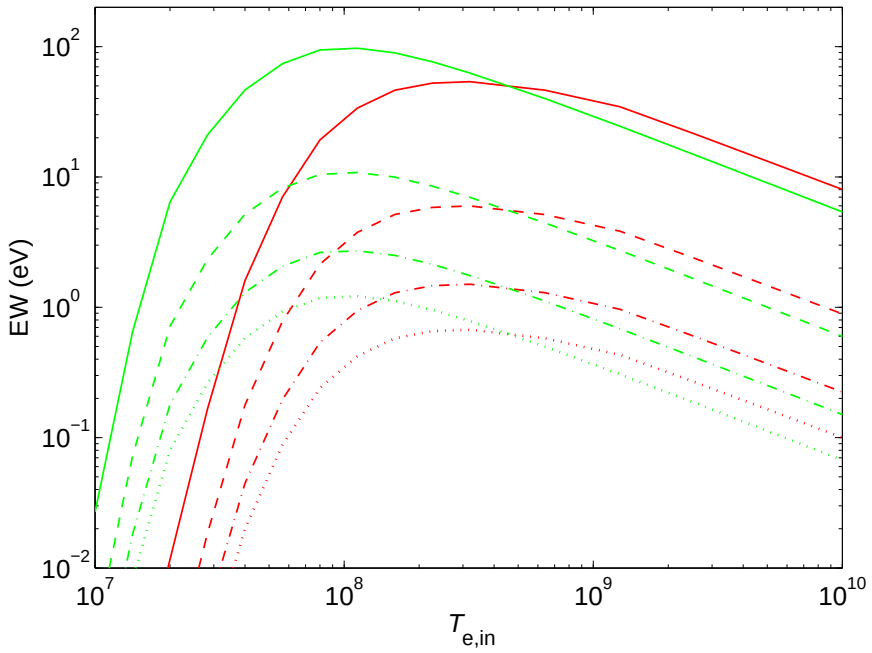

Fig. 5.— The equivalent widths of the line emitted from the outflows as functions of the electron temperature at the base of the outflow. The black hole mass $M_{\rm bh} = 10M_{\odot}$, the accretion power $L_{\rm acc} = P_{\rm kin} = 10^{39}$ erg s^{-1}, and the outflow velocity $\beta_{\rm j} = 0.3$, are adopted in the calculations. The red lines are the luminosities of the Fe XXVI Kα emission line for the outflows, while the green lines are the Fe XXV Kα emission line luminosity. The different types of the lines represent the results calculated with the different opening angle of the outflow (solid lines: $\theta_{\rm j} = 5°$; dashed lines: $\theta_{\rm j} = 15°$; dash-dotted lines: $\theta_{\rm j} = 30°$; dotted lines: $\theta_{\rm j} = 45°$).